Journal of Thermal Analysis and Calorimetry (2019) 137:2115–2120
https://doi.org/10.1007/s10973-019-08106-x

Phase equilibria in the CeI_3–CsI binary system

A. Dańczak[1] · L. Rycerz[1]

Received: 14 July 2018 / Accepted: 15 February 2019 / Published online: 2 March 2019

Abstract
The phase equilibria in the cerium(III) iodide–cesium iodide pseudobinary system were established by differential scanning calorimetry. The system is characterized by existence of three compounds: Cs_3CeI_6, $Cs_3Ce_2I_9$ and $CsCe_2I_7$. First one, namely Cs_3CeI_6, melts congruently at 823 K and undergoes two phase transitions at 658 and 762 K. Second compound, Cs_3CeI_6, decomposes in the solid state at 610 K. The last existing compound, $CsCe_2I_7$, melts incongruently at 826 K. The eutectics composition was found from Tammann plot, which predicts, through application of the lever rule, the variation of the enthalpy associated with eutectic melting as a function of composition. The composition of CsI–Cs_3CeI_6 and Cs_3CeI_6–$CsCe_2I_7$ eutectics corresponds to cerium(III) iodide mole fraction $x = 0.127$ ($T = 823$ K) and $x = 0.485$ ($T = 737$ K), respectively.

Keywords Phase diagram · Cerium(III) iodide · Cesium iodide · DSC

Introduction

Rare-earth halides have a significant impact on modern technologies and are used in a number of applications such as reprocessing of nuclear wastes, recycling of spent nuclear fuel [1] doses in high-intensity discharge lamps, lasers and new highly efficient light sources with energy-saving futures [2, 3]. The lanthanide halides are used extensively in metal halide discharge lamps [4, 5]. They enable the design of light sources with good-quality white light spectral output and high color rendering properties at high efficacies.

Application of rare-earth halides in numerous areas of modern technology requires knowledge of their thermochemical properties. For example, a ceramic metal halide discharge lamp is based on combination of the iodides of sodium, thallium together with a mixture of lanthanides [6]. Light is produced by radiation from excited mercury atoms and from such iodides in the gas phase. The relative amounts of the metallic halides affect the efficacy, color appearance and color rendition of the light source. In order to understand this behavior, it is necessary to understand the thermodynamics and vaporization properties of a variety of alkali metal–lanthanide metal iodide systems. These allow the calculation of partial pressures above a liquid mixture and are therefore of considerable importance in modeling the behavior of metal halide discharge lamps. The thermodynamic data are also indispensable for predicting the behavior of doses by modeling multicomponent metal halide system [7].

Numerous studies have been carried out to investigate thermochemistry of rare-earth chlorides and bromides and their binary systems with the alkali halides [8–18]. However, the knowledge of rare-earth iodides is still scanty. The data about these iodides and their systems with alkali iodides are incomplete and contradictory. Some information about thermodynamic properties of pure rare-earth iodides is available in the literature: DyI_3 [19], CeI_3 [13, 20, 21], LaI_3 [20–22] and NdI_3 [13, 20]. Additionally, the enthalpies of lanthanide iodides formation are presented in the work of Cordfunke and Konings [23]. The phase equilibria in LnI_3–MI binary systems (Ln = La, Pr, Nd, Sm, Gd, Dy, Er; M = Na, K, Cs) were investigated by Kutscher and Schneider [10]. The phase diagrams of LaI_3–RbI and NdI_3–RbI were determined by Rycerz [13]. Existence of M_3LnI_6 compound (M = K, Rb, Cs), which melts congruently, was evidenced in all these systems,

✉ A. Dańczak
anna.danczak@pwr.edu.pl

[1] Division of Analytical Chemistry and Analytical Metallurgy, Faculty of Chemistry, Wrocław University of Science and Technology, Wybrzeże Wyspiańskiego 27, 50-370 Wrocław, Poland

except for the LaI_3–KI system. The LaI_3–KI system is characterized only by existence of K_2LaI_5 compound which melts congruently [10]. There is no experimental thermodynamic data concerning the CeI_3–MI (M = Li, Na, K, Rb, Cs) binary systems.

The phase diagram of CeI_3–CsI binary system was determined in this work for the first time. In the literature, only calculated phase diagram of the same system can be found [6]. According to these calculations, three compounds, namely Cs_3CeI_6, $Cs_3Ce_2I_9$ and $CsCe_9I_{28}$, occur in this system. One of them, $CeCs_3I_6$, undergoes solid–solid phase transition and melts congruently at temperatures of about 760 K and 950 K, respectively (temperatures estimated from the graphical phase diagram). Second compound, $Cs_3Ce_2I_9$, decomposes in the solid phase at temperature of about 680 K. Third compound, $CsCe_9I_{28}$, melts incongruently at 810 K. However, the stoichiometry of this compound, $CsCe_9I_{28}$, seems unusual and doubtful. Existence of such compounds was not evidenced in existing LnI_3–MI binary systems. Therefore, we decided to reinvestigate the phase equilibria in the CeI_3–CsI binary system. This article is the first work focused on the experimental determination of the CeI_3–CsI phase diagram.

Experimental

Chemical and samples preparation

Cerium(III) iodide and cesium iodide were Alfa Aesar and Sigma-Aldrich reagents with purity of 99.9%. They were handled inside a high purity argon atmosphere in a glove box (water content < 2 ppm). The CeI_3 and CsI mixtures (in appropriate proportions weighed with precision of about 1 mg) were prepared in vacuum-sealed quartz ampoules and melted in electric furnace. After homogenization and solidification, these samples were ground in an agate mortar in a glove box and transferred to the DSC quartz cells. Different compositions prepared in this way were used in phase diagram measurements.

Measurements

A Setaram Labsys Evo 1600 differential scanning calorimeter (DSC) was used to investigate the phase equilibria in the CeI_3–CsI binary system. Experimental samples (150–350 mg) were kept in vacuum-sealed quartz ampoules with a diameter of 6 mm and a length of 15 mm. The DSC investigations on samples with 26 compositions were conducted with heating and cooling rates 5 K min^{-1}. Data acquisition and processing were computer operated using CALISTO Thermal Analysis Software. The apparatus was calibrated by the Joule effect. The same quartz cells as for enthalpy of phase transitions measurements were used. Four standards (Ag, Bi, Cd. Sn, Sb, Zn) with their melting temperature within the desired temperature range (473–1373 K) and with purity 99.99% were chosen for calibration process. Other experimental conditions were set to values that were used in sample analysis, in particular: sensor type, crucible material, argon flow, heating and cooling rate. The maximum relative experimental error on enthalpy of phase transition did not exceed 3%. Temperature was measured with precision ± 1 K.

On the DSC cooling curves of all samples, the supercooling effect was observed (Fig. 1). The temperature values of all phase transitions determined from the cooling curves were from several to several tens Kelvin lower than the same values determined from the DSC heating curves. In all heating runs, the temperature of maximum of the peak at the highest temperature corresponds to the liquidus temperature. In all the other cases, onset temperature (T_{onset}) was assumed as the effect temperature.

Results and discussion

The analysis of the DSC curves was performed with Setaram Calisto software, which also allowed separating overlapped peaks. The example of thermal effects overlapping is presented in Fig. 1, where effect related to the eutectic is overlapped by liquidus effect. In order to determine enthalpy related to eutectic effect, the deconvolution of the overlapping peaks was conducted by Calisto software. The results of deconvolution are displayed in Fig. 2. The total enthalpy corresponding to both overlapped peaks was determined as 19.4 kJ mol^{-1}, and it was unclear which part of this enthalpy is related to the eutectic. After peak separation, it was evident that the enthalpy corresponding to the eutectic was equal to 11.2 kJ mol^{-1}.

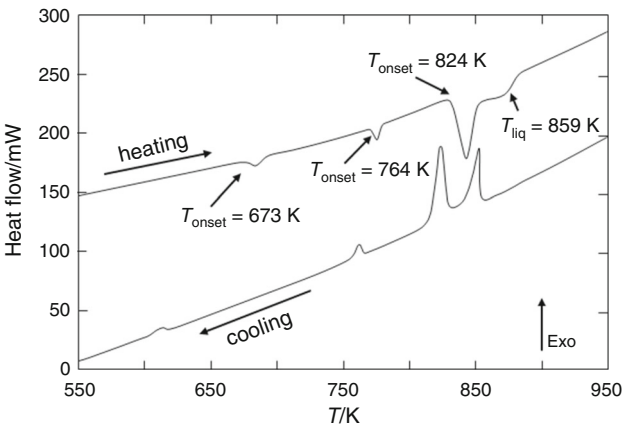

Fig. 1 DSC curve of the CeI_3–CsI mixture with composition $x(CeI_3) = 0.102$

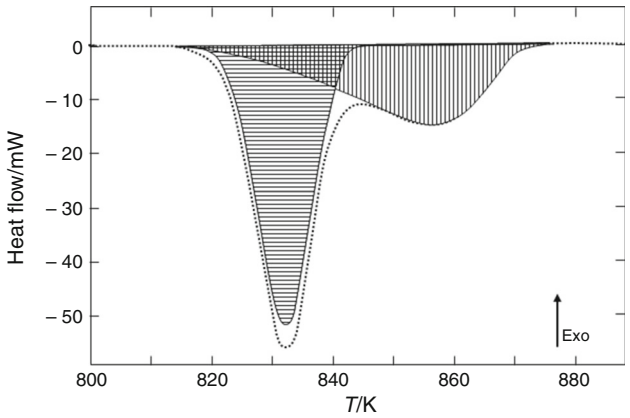

Fig. 2 Fragment of DSC curve of the sample with composition $x(CeI_3) = 0.102$ after separation method

The remaining enthalpy (7.9 kJ mol^{-1}) was connected with liquidus effect.

It was established that pure cerium(III) iodide melts at 1031 K. This temperature is in excellent agreement with the literature data 1033 K [13, 20, 21]. The melting temperature of pure cesium iodide was found to be 909 K, which is also in good agreement with the literature data 905 K [21].

Some characteristic DSC heating curves are presented in Figs. 1 and 3. Two, four or five endothermic effects were observed on these curves dependently on composition of the samples. The effect at the highest temperature corresponds, as stated previously, to the liquidus temperature.

In the composition range $0 < x < 0.250$, where x is CeI_3 mol fraction, three additional endothermic effects were observed in addition to the liquidus effect (Fig. 1). The first one, observed at 823 K (average value from measurements of different samples), disappears at $x = 0.250$. This suggests existence of Cs_3CeI_6 compound. Accordingly, it can be ascribed to the CsI–Cs_3CeI_6 eutectic. The eutectic composition was determined from the Tammann plot (Fig. 4a) as $x = 0.127 \pm 0.007$. The mixture with eutectic composition melts with enthalpy, $\Delta_{fus}H_m$, of 14.4 ± 0.8 kJ mol^{-1}.

The second thermal effect, at 762 K (average value from the measurements), was observable in all the curves up to $x = 0.450$, the composition at which it disappeared. The maximum enthalpy related to this effect (3.1 ± 0.3 kJ mol^{-1}), determined from Tammann diagram (Fig. 4b), corresponds to the mole fraction of cerium(III) iodide $x = 0.270 \pm 0.018$ which is in good agreement with stoichiometry of the Cs_3CeI_6 compound ($x = 0.250$). This effect can be ascribed to the phase transition of Cs_3CeI_6 compound.

The third thermal effect at 658 K (average value from experiments) was observed on curves of samples with x up to 0.666. Its disappearance for samples with $x \geq 0.666$

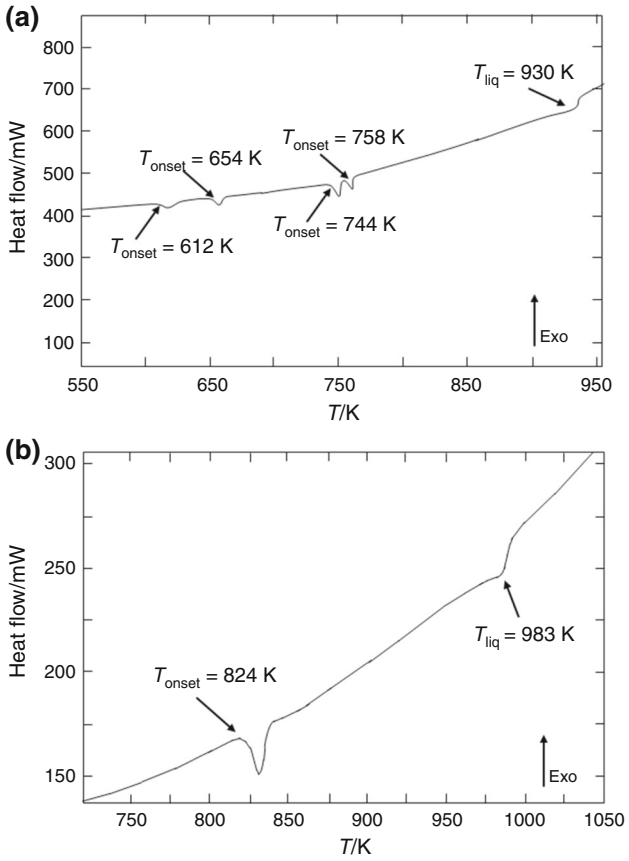

Fig. 3 DSC curves of the CeI_3–CsI mixtures with different compositions: **a** $x(CeI_3) = 0.327$ and **b** $x(CeI_3) = 0.849$

suggests existence of another compound ($CsCe_2I_7$) in the investigated system. Tammann diagram, i.e., dependence of the enthalpy related to this effect on the composition, is presented in Fig. 4c. The maximum of enthalpy (3.05 ± 0.20 kJ mol^{-1}) determined from the intercept of two liner parts on the Tammann plot corresponds to the mole fraction of cerium(III) iodide $x = 0.279 \pm 0.023$. This value is in a quite good agreement with stoichiometry of Cs_3CeI_6 compound. It means that Ce_3CeI_6 is formed or undergoes another phase transition at 658 K. Taking into account the enthalpy value related to the effect at 658 K, calculated per one mole of Ce_3CeI_6 compound (12.20 kJ mol^{-1}), it can assume that this effect does not correspond to its formation but to phase transition. Comparison of molar enthalpy corresponding to the phase transitions of M_3LnCl_6, M_3LnBr_6 and M_3LnI_6 compounds [13] leads to very interesting conclusion. Formation of the M_3LnX_6 compounds from M_2LnX_5 and MX, where X = Cl, Br and I (reconstructive phase transition), is associated with large enthalpy changes (27–55 kJ mol^{-1}), while structural transitions (non-reconstructive phase transitions) in these compounds are associated with significantly lower enthalpy changes (8–12 kJ mol^{-1}). The

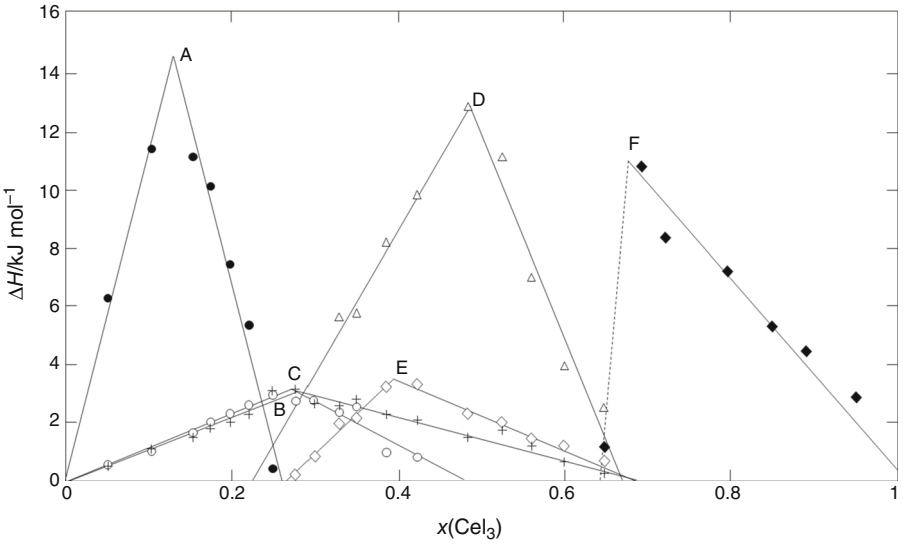

Fig. 4 Tammann diagrams, constructed on the basis of experimentally determined enthalpy: **a** CsI–Cs_3CeI_6 eutectic, **b** phase transition of Cs_3CeI_6 compound, **c** phase transition of Cs_3CeI_6 compound, **d** Cs_3CeI_6–$CsCe_2I_7$ eutectic, **e** decomposition of $Cs_3Ce_2I_9$ and **f** incongruent melting of $CsCe_2I_7$

Table 1 Results of the DSC experiments performed on the CeI_3–CsI binary system

$x(CeI_3)$	Temperature/K						
	Cs_3CeI_6 phase transition	Cs_3CeI_6 phase transition	CsI–Cs_3CeI_6 eutectic	$Cs_3Ce_2I_9$ decomposition in solid state	Cs_3CeI_6–$CsCe_2I_7$ eutectic	$CsCe_2I_7$ incongruent melting	Liquidus
0.000	–	–	–	–	–	–	909
0.049	675	764	824	–	–	–	884
0.102	673	764	824	–	–	–	859
0.150	666	763	822	–	–	–	836
0.173	670	764	825	–	–	–	858
0.197	670	764	823	–	–	–	914
0.220	672	765	823	–	–	–	933
0.254	669	764	821	–	–	–	952
0.276	653	764	–	610	–	–	940
0.298	647	760	–	607	–	–	946
0.327	654	758	–	612	744	–	930
0.349	654	759	–	614	738	–	931
0.385	650	756	–	611	739	–	899
0.422	648	757	–	613	733	–	881
0.484	654	–	–	612	742	–	757
0.525	645	–	–	609	731	–	754
0.559	645	–	–	613	736	–	781
0.599	649	–	–	604	736	–	817
0.648	649	–	–	609	730	824	834
0.696	–	–	–	–	–	826	865
0.719	–	–	–	–	–	825	891
0.797	–	–	–	–	–	825	955
0.849	–	–	–	–	–	824	983
0.891	–	–	–	–	–	827	993
0.954	–	–	–	–	–	829	1015
1.000	–	–	–	–	–	–	1031

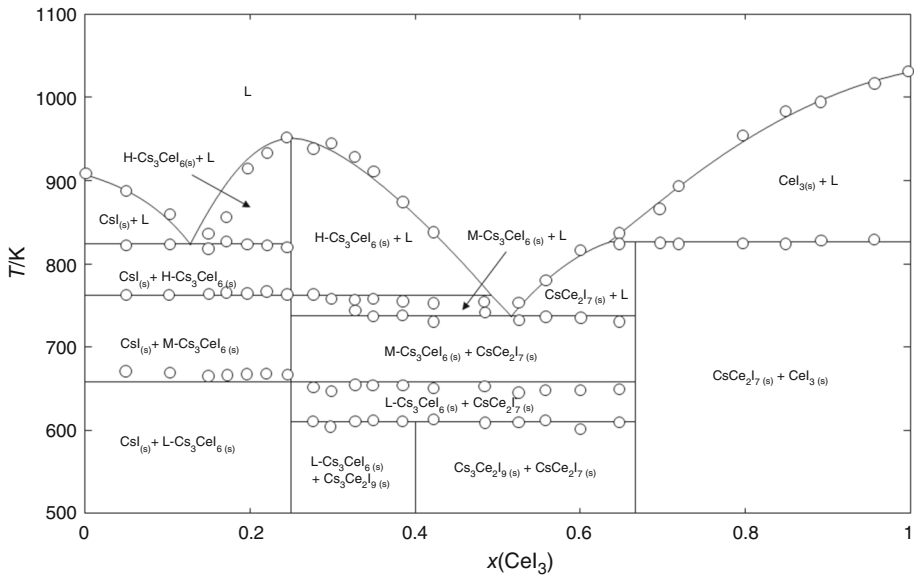

Fig. 5 Phase diagram of CeI_3–CsI binary system

small enthalpy of effect at 658 K (12.20 kJ mol^{-1}) suggests that this effect corresponds to structural transition (transition from low-to-middle temperature modification of Cs_3CeI_6 compound).

In the composition range $0.250 < x < 0.666$, two new thermal effects were observed in addition to the liquidus and described above effects at 762 K and 658 K related to the phase transition of Ce_3CeI_6 compound (Fig. 3a). Their disappearance at $x = 0.666$ suggests existence of $CsCe_2I_7$ compound. First of them, at 737 K (average value), can be ascribed to the Cs_3CeI_6–$CsCe_2I_7$ eutectic. The eutectic composition $x(CeI_3) = 0.485 \pm 0.013$ is determined from Tammann plot shown in Fig. 4d. The mixture with eutectic composition melts with enthalpy, $\Delta_{fus}H_m$, of about 12.88 ± 0.21 kJ mol^{-1}.

Second effect was observed at temperature 610 K. Determining from the Tammann plot (Fig. 4e), maximum value of enthalpy (3.45 ± 0.18 kJ mol^{-1}) related to this effect corresponds to the molar fraction of cerium(III) iodide $x = 0.391 \pm 0.011$. This value is in quite good agreement with stoichiometry of $Cs_3Ce_2I_9$ compound. Accordingly, effect at 610 K can be ascribed to the decomposition of $Cs_3Ce_2I_9$ in the solid phase.

In the composition range $0.666 < x < 1$, only one endothermic effect, at 826 K, was observed in addition to the liquidus (Fig. 3b). It is undoubtedly related to the incongruent melting of new compound. Tammann diagram constructed for this effect shown in Fig. 3f gave the mole fraction of cerium(III) iodide $x = 0.667 \pm 0.023$ which is in excellent agreement with stoichiometry of mentioned above $CsCe_2I_7$ compound.

All the experimental data are presented in Table 1, and the complete phase diagram is shown in Fig. 5.

In comparison with the literature data [6], our finding confirmed existence of only $CeCs_3I_6$ and $Cs_3Ce_2I_9$ compounds. We found no evidence of the existence of $CsCe_9I_{28}$ compound. Instead we found another compound, $CsCe_2I_7$, which melts incongruently at 826 K. In the case of Cs_3CeI_6 compound, our results are in a good agreement with the literature data for solid–solid phase transition (762 K and 770 K) and congruent melting (952 K and 950 K). However, we found another solid–solid phase transition of this compound at 658 K, which was not evidenced by the literature data. Significant difference between the literature data [6] and our finding concerns also the temperature of $Cs_3Ce_2I_9$ decomposition in the solid phase (680 K and 610 K, respectively). Some differences can be found additionally in the composition and temperatures of eutectics. According to our results, CsI–Cs_3CeI_6 eutectic appears at mole fraction of CeI_3 equal 0.127 and melts at 823 K, whereas according to the literature, these values are 0.100 and 815 K, respectively. The same data for Cs_3CeI_6–$Cs_3Ce_2I_9$ eutectic are 0.485 and 737 K and 0.50 and 760 K, respectively.

In the literature, one can find some information concerning these compounds. According to [24], the crystal structure of Cs_3CeI_6 is not known, but from the systematics of the binary compounds one can be quite certain that it exhibits octahedral surrounding of the cerium cations. This assumption was confirmed by Raman spectroscopy. The same authors inform about phase transition in Cs_3DyI_6 at temperature about 757 K and expect the same in Cs_3CeI_6 compound. Indeed, we found this transition at 762 K. The existence of Cs_3CeI_9 was confirmed also by Raman spectroscopy [24]. Unfortunately, its crystal structure is unknown.

The existence of definite compounds in the system under investigation should be confirmed by XRD measurements. However, due to extreme hygroscopicity of CeI_3 and its mixtures, the standard measurements were unsuccessful. We hope to perform these measurements in the future with using quarts capillaries.

Conclusions

1. Phase equilibria in the CeI_3–CsI binary system were established experimentally for the first time. Three stoichiometric compounds exist in this system. First (Cs_3CeI_6) undergoes two phase transitions at 658 K and 762 K and melts congruently at 952 K. Second ($Cs_3Ce_2I_9$) decomposes in the solid phase at 610 K. Third compound ($CsCe_2I_7$) melts incongruently at 826 K.
2. Construction of the Tammann diagrams was very useful in determination of eutectics composition. CsI–Cs_3CeI_6 and Cs_3CeI_6–$CsCe_2I_7$ eutectics were found to be located at $x = 0.127$ (823 K) and 0.485 (737 K), respectively.
3. The CeI_3–CsI binary system phase diagram determined in this work differs from the calculated diagram available in the literature. Experimental phase diagram of investigated system shows the existence of the new $CsCe_2I_7$ compound that was not evidenced in the literature data. Existence of $CsCe_9I_{28}$ compound postulated in the literature was not confirmed by the experimental studies.

Acknowledgements The work was co-financed by a statutory activity subsidy from Polish Ministry of Science and Higher Education for the Faculty of Chemistry of Wroclaw University of Science and Technology.

References

1. Naumov VS, Bychkov AV, Lebedev A. Advenctes in molten salts: from structural aspects to waste processing. In: Gaude-Escard M, editor. Properties of liquid-salt nuclear fuel and its reprocessing technology. Danbury: Begell House Inc; 1999. p. 432–53.
2. Junming T, Bath NY. Quarty metal halide lamp with improved lumen maintenance. U.S. Patent Application Publication; 2008. US2008/0093993 Ai.
3. Junming T, Bath NY. Quarty metal halide lamp with improved lumen maintenance. U.S. Patent Application Publication; 2010. US 7,786,674 B2.
4. Brooker MH, Papatheodorou GN. In: Mamantov G, editor. Advances in molten salt chemistry, vol. 5. New York: Elsevier; 1983. p. 27.
5. Hilpert K. Complexiaton in metal halide vapors—a review. J Electrochem Soc. 1989;136:2099.
6. Dinsdale A, Davies RH, Mucklejohn SA. Thermodynamic data for the (NaI–CeI_3) and (CsI–CeI_3) systems in the condensed and gas phases. J Light Vis Environ. 2013;37(4):156–65.
7. Guest EC, Mucklejohn SA, Preston B, Rouffet JB, Zissis G. NumeLiTe: an energy effective lighting system for roadways and an industrial application of molten salts. In: Oye HA, Jagtoyen A, editors. Proceedings of international symposium on ionic liquids in honour of M. Gaune-Escard, Carry le Rouet, France; 2003. pp. 26–28, 37–45.
8. Prosypajko VI, Alekseeva EA. In: Bell HB, editor. Phase equilibria in binary halides. New York: IFI/Plenum; 1987.
9. Vogel Von G. Untersuchung der Zustandsdagramme von Lanthanidenbromiden in Gemisch mit Alkalibromiden. Z Anorg Allg Chem. 1972;388:43–52.
10. Von Kutscher J, Schneider A. Zur Systematik der Zustandsdiagramme von Lanthaniden(III)-halogenid-Alkalihalogenid-Systemen. Z Anorg Allg Chem. 1974;408:135–45.
11. Blachnik R, Selle D. Zur Thermochemie von Alkalichlorid-Lanthanoid(III)-chloriden. Z Anorg Allg Chem. 1979;454:90–8.
12. Seifert HJ. Ternary chlorides of the trivalent early lanthanides:phase diagrams, crystal structures and thermodynamic properties. J Therm Anal Calorim. 2002;67:789–826.
13. Rycerz L. Thermochemistry of lanthanide halides and compounds formed in lanthanide halide–alkali metal halide systems. Wrocław: Scientific Papers of Institute of Inorganic Chemistry and Metallurgy of Rare Elements. Wroclaw University of Technology; 2004. p. 35.
14. Seifert HJ. Ternary chlorides of the trivalent late lanthanides: phase diagrams, crystal structures and thermodynamic properties. J Therm Anal Calorim. 2006;83:479–505.
15. Bounouri Y, Berkani M, Zamouche A, Dańczak A, Chojnacka I, Rycerz L. Thermodynamic properties of the $NdBr_3$–MBr binary systems (M = Na, K). J Therm Anal Calorim. 2018;133:1589–96.
16. Dańczak A, Salamon B, Kapała J, Rycerz L, Gaune-Escard M. Reinvestigation of phase equilibria in $TbCl_3$–LiCl binary system. J Therm Anal Calorim. 2017;130:25–33.
17. Dańczak A, Rycerz L. Reinvestigation of the $DyCl_3$–LiCl binary system phase diagram. J Therm Anal Calorim. 2016;126(1):299–305.
18. Salamon B, Rycerz L, Kapała J, Gaune-Escard M. Phase diagram of NdI_3–RbI pseudo-binary system. Thermodynamic properties of solid compounds. J Phase Equilib. 2015;404:9–16.
19. Groen CP, Cordfunke EHP, Huntelaar ME. The thermodynamic properties of $DyBr_3$(s) and DyI_3(s) from T = 5 K to their melting temperatures. J Chem Thermodyn. 2003;35:475–92.
20. Dworkin AS, Bredig MA. Enthalpy of lanthanides chlorides, bromides and iodides from 298-1300.deg.K: enthapies of fusion and transition. High Temp Sci. 1971;3(1):81–90.
21. Kubaschewski O, Alcock CB, Spencer PJ. Materials thermochemistry. 6th ed. Oxford: Pergamon Press; 1998.
22. Wicks C, Block FE. Thermodynamic properties of 65 elements. U S Bur Mines Bull. 1963;605:67.
23. Cordfunke EHP, Konings RFM. The enthalpies of formation of lanthanide compounds I. $LnCl_3$(cr), $LnBr_3$(cr) and LnI_3(cr). Thermochim Acta. 2001;375:17–50.
24. Chrissanthopoulos A, Zissi GD, Papatheodorou GN. The structure of molten rare-earth iodide-alkali iodide mixtures. Z Naturforsch. 2005;60a:739–48.